Table 1 Summary of parachute test data

Parachute		Range of test conditions		
Type	Geometry	v_s, fps	q_s, lb/ft^2	Ref.
Flat circular	3-ft D_0, 28-gore	50–85	3–8.5	6
Flat circular	28-ft D_0, 28-gore	154–288	18.6–50.6	7[a]
Flat circular	100-ft D_0, 120-gore, single-reefed stage	263–324	76–116	8
Conical	95-ft D_0, 108-gore, single-reefed stage	218–454	53–227	8

[a] Four tests reported by Berndt in which the chute squidded at $v_s >$ 300 fps are omitted.

Test Data

Figure 1 shows the suggested plot of F_0/q_sS_0 vs v_st_f/D_0. In the figure, the values of v_st_f/D_0 at $F_0/q_sS_0 = 1.5$ correspond to the infinite mass case and were calculated from infinite mass filling time formulas for solid, flat circular chutes[3,4] with assumed effective porosity values of 0.03–0.05. The remaining points in the figure are from the test data summarized in Table 1. As noted, the 95-ft and 100-ft D_0 chutes were used with reefing, so there is some doubt if data for these chutes are really suited to comparison with unreefed chute data. However, for very large chutes reefing appears to assist symmetry of inflation more than it affects opening load or time. In addition, only those 95-ft and 100-ft D_0 chute tests in which opening force upon inflation to full blossom was greater than opening force upon inflation to reefed stage were used for Fig. 1.

Discussion

The data of Fig. 1 confirm that the parachute inflation process is subject to relatively large dispersion, yet remain well ordered enough to be amenable to empirical curve-fitting techniques. That is, if a satisfactory method can be found for calculation of t_f, data as in Fig. 1 will permit the empirical calculation of F_0 and its tolerances for the given value of t_f.

In this Note, only test data with good reporting of test variables were used. However, earlier test data on 24-ft D_0 solid, flat circular chutes have been examined and found to exhibit the same trend as in Fig. 1, although with larger scatter. Data summarized by Walcott[9] on 35, 56, and 64-ft D_0 10% extended-skirt-type parachutes likewise show the same trend as Fig. 1, but with a lower value of F_0/q_sS_0 for a given value of v_st_f/D_0, as would be expected.

It appears that useful information on the parachute opening process and its statistics can be obtained by plotting F_0/q_sS_0 vs v_st_f/D_0 for various types of parachute and by correlating the resulting data with empirical curve-fitting techniques. Figure 1 shows that some additional test data for solid, flat circular parachutes are desirable in the ranges $1.5 > F_0/q_sS_0 > 0.45$ and $0.08 > F_0/q_sS_0 > 0.025$. Test conditions required to obtain such data can be established on the basis of available scaling laws.[1]

References

[1] French, K. E., "Model Law for Parachute Opening Shock," *AIAA Journal*, Vol. 1, No. 11, Nov. 1963, pp. 2226–2228.

[2] French, K. E., "Comment on 'A Method for Calculating Parachute Opening Forces for General Deployment Conditions,'" *Journal of Spacecraft and Rockets*, Vol. 4, No. 10, Oct. 1967, pp. 1407–1408.

[3] "Performance of and Design Criteria for Deployable Aerodynamic Decelerators," ASD-TR-61-579, Dec. 1963, Flight Dynamics Lab., Wright-Patterson Air Force Base, Ohio, p. 163.

[4] Heinrich, H. G., "Opening Time of Parachutes Under Infinite Mass Conditions," *Journal of Aircraft*, Vol. 6, No. 3, May–June 1969, pp. 268–272.

[5] Berndt, R. J. and DeWeese, J. H., "Filling Time Prediction Approach for Solid Cloth Type Parachute Canopies," *Proceedings of the 1st Aerodynamic Decelerator Systems Conference*, AIAA, New York, 1966, pp. 17–32.

[6] Heinrich, H. G. and Noreen, R. A., "Analysis of Parachute Opening Dynamics with Supporting Wind Tunnel Experiments," AIAA Paper 68-924, El Centro, Calif., 1968.

[7] Berndt, R. J., "Experimental Determination of Parameters for the Calculation of Parachute Filling Times," *Jahrbuch 1964 der WGLR*, Vieweg und Sohn, Braunschweig, Germany, 1965, Table 1, p. 305.

[8] Gimalouski, E. A., "Development of a Final Stage Recovery System for a 10,000 Pound Weight," WADC TR 59-109, Dec. 1958, Wright-Patterson Air Force Base, Ohio.

[9] Walcott, W. B., "Study of Parachute Scale Effects," ASD-TDR-62-1023, Jan. 1963, Air Force Systems Command, Wright-Patterson Air Force Base, Ohio.

Evaluation of a Quartz-Fiberfrax Heat Shield at High Radiative Heating Rates

G. F. Greenwald* and V. A. Corea†
McDonnell Douglas Astronautics Company, Santa Monica, Calif.

Introduction

THE present Thor booster configuration has three solid strap-on motors that burn during the first 40 sec of flight. The proposed addition of extra solid motors to the Thor booster (up to a total of nine motors in its most advanced configuration) increases the heating rates to the base region beyond the present capability of the insulation system to protect the many items of base hardware.

A testing program was initiated to screen several candidate materials of both ablative and insulative types to replace or augment the existing insulation system. One material, viz. a sandwich of quartz cloth and Fiberfrax felt, significantly outperformed all of the other materials tested.

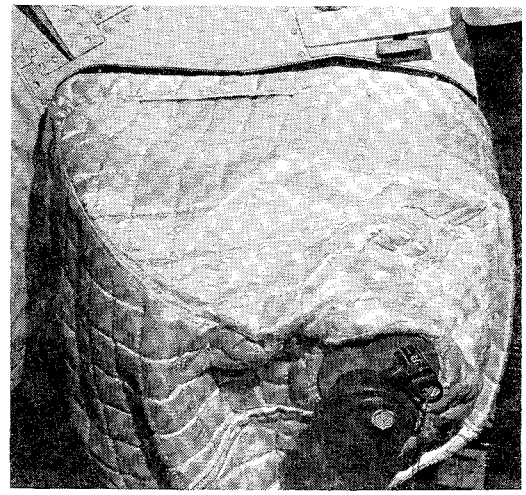

Fig. 1 Installed heat shield.

Received July 16, 1969. This Note is based on work performed by the McDonnell Douglas Astronautics Company, Western Division, under NASA Contract NAS7-545. The authors are indebted to M. C. Coes, McDonnell Douglas Astronautics Company, Western Division, for her assistance in selecting the materials for the tests.

* Senior Engineer/Scientist, Delta Aero/Thermodynamics Section, Flight Mechanics Branch, Development Engineering, Western Division. Member AIAA.

† Engineer/Scientist Specialist, Delta Aero/Thermodynamics Section, Western Division.

Table 1 Thermal conductivities of fiberfrax

Temperature, °F	Thermal conductivity, Btu/ft hr °F
400	0.38
800	0.61
1200	0.98
1600	1.47
1800	1.73

The material system is very lightweight (less than 10 lb/ft^3), has low conductivity, and can withstand very high heating rates (tested at 50 Btu/ft^2 sec for 40 sec) with no apparent degradation. In addition, its relatively high strength, flexibility and formability (as compared to other refractory materials) make it suitable for a number of applications where a nonablative external heat shield is desired, especially where flexing occurs during the period of high heating. The closure around a gimballed rocket engine is an example of such an application; it is the primary proposed use for the material (see Fig. 1).

This Note describes the results of the tests and presents an analytical model that has been developed to predict the back face temperature of the insulation.

Material

The selected insulation is a fibrous high-purity alumina-silica (made by Carborundum under the trade name of Fiberfrax Lo-Con blanket) of various thicknesses sandwiched between two layers of quartz woven cloth (Astroquartz 581 with a 9073 finish).[1] The Fiberfrax blanket has an approximate composition[2] by weight of 50.9% Al_2O_3, 46.8% SiO_2, 1.2% B_2O_3, and 0.8% Na_2O; trace inorganics account for 0.3 to 0.5%. The material is said to have excellent chemical stability, with good resistance to most chemicals except hydrofluoric and phosphoric acids and strong alkalies. The material has a density of 6 lb/ft^3, a specific heat of 0.27 Btu/lbm°F, and its thermal conductivities at various temperatures are indicated in Table 1.

Test Description

The material performance was evaluated by heating with a bank of tungsten filament quartz lamps, controlled to simulate the predicted flight heating rate histories. The samples were rectangular, 6 in. × 8 in., mounted vertically with the front face nominally 2½ in. from the lamps. The back surface of each specimen was instrumented with at least one thermocouple; these were attached by either sewing to the back face with quartz thread or by weaving into the cloth. Directly beneath the sample was a water-cooled calorimeter (Hy-Cal-C-1300-A-072) which was used as a feed-back device to control the lamps. During the test the samples were flexed by a motor-driven arm that raised the lower end of the specimens by one inch, at a rate of 45 cycles per minute.

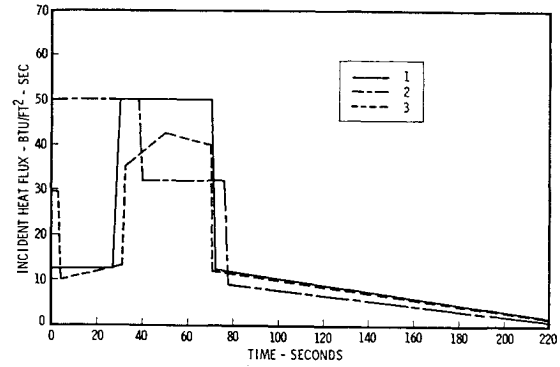

Fig. 2 Applied heating rates.

The heating rate histories used in the test are shown in Fig. 2. These heating rates represent predicted values for the six-solid-motor and nine-solid-motor configurations.

Discussion of Test Results

The maximum back-face temperatures achieved during the various tests are summarized in Table 2, and a typical time-temperature trace is shown in Fig. 3.

The performance of the material in the high heat flux environment is rather remarkable. With two exceptions the post-test samples were indistinguishable with regard to appearance and physical properties from the pretest material. The two exceptions were sample 9, where silicone rubber was used on the outer surface with no apparent detrimental effect on the substrate fabric, and sample 5, where a silicone rubber adhesive was used on the threads; the latter material caused severe contamination of the surface, resulting in an increased absorptivity, and embrittlement of the quartz (Fig. 4). On the other hand, attempts at purposeful contamination with carbon black (sample 2) had no noticeable effect. Within seconds, the carbon burned off, leaving the characteristic white surface during the remainder of the test.

Since exposure to rain or launch-pad deluge was a real possibility, a water-soaked sample was tested (sample 3) with no detrimental effect. As expected, the sample was still wet after the test, and remained very cool during heating. The water absorption raised the pretest weight 500% over the dry samples.

Table 2 Test results

Sample	Sewing pattern	Heating rate curve no.	Thermocouple mounting	Maximum back-face temperature, °F	Comments
½ in. Fiberfrax					
1	not sewn	1	sewn	490	
2	not sewn	1	sewn	485	Front layer coated with carbon black
3	not sewn	1	sewn	155	Soaked in water prior to test
4	1-in. grid	1	sewn	620	
5	2½-in. grid	2	woven, sewn	970 965	Silicone rubber adhesive on 50% of specimen
6	2½-in. grid	2	woven	650	
7	2½-in. grid	2	woven	637	
8	2½-in. grid	3	woven	522	
¾ in. Fiberfrax					
9	not sewn	1	sewn	535	Had extra layer of silicone rubber-coated quartz cloth on front
10	2½-in. grid	2	woven	495	

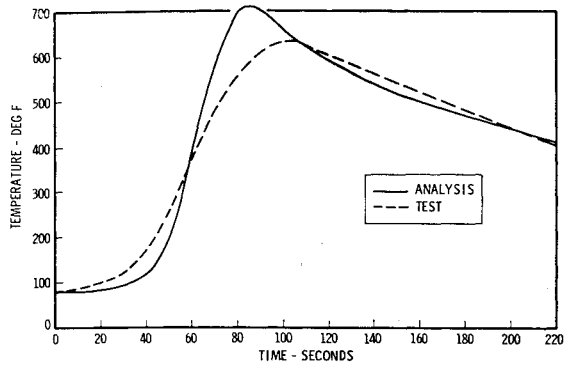

Fig. 3 Test specimen back-face temperature history.

Some of the effects of compression due to sewing can be seen by comparison of the maximum temperature on samples 1 and 4. What is not indicated is the temperature at or near the threads, where more than average compression occurs; on some samples these areas were found to be as much as 400°F hotter than the temperatures midway between the threads.

In general it has been found advisable to sew the material with as little local compression in the thread area as possible. This precaution results both in reduced temperatures in the thread area and better wear resistance of the material.

The effect of increasing the nominal Fiberfrax thickness results in a decrease in the temperature of the back surface, as seen by comparison of temperatures on samples 6, 7, and 10.

Analysis

Proper applications of the material require an analytical model with which the temperature behavior of the material in use can be predicted with some confidence. In this instance, the analytical model considered a heat source to the front face of the test sample of a value determined by the calorimeter measurement. The level of the heat source is reduced by the absorptivity[3] of the quartz cloth at 0.95 μ wave length 0.585. The front face is assumed to radiate with emissivity[4] 0.68 and convect to the surroundings at a constant nominal temperature. Likewise, the back face is assumed to radiate, with emissivity 0.92, and convect to the same environment as the front face. The point is that it is important to account for spectral variations in surface radiation properties and that the published surface properties of pure quartz fit the behavior of the Astroquartz satisfactorily. Standard finite-difference techniques were applied to the transient heat conduction equation for the thermal history prediction of the blanket. A comparison of analytical and test results appears in Fig. 3. The peak temperatures are predicted within 10% based on temperature rise, and the final temperatures are predicted within 10 deg.

Conclusions

The low-density sandwich of quartz cloth and Fiberfrax filler is an excellent heat shield for high radiative heating rate applications, especially where flexing is necessary during heating. Generally, it is recommended that the surface be kept clean of any "protective" coatings, such as silicone rubber, since such materials may have a detrimental effect on the heat shield performance (see charred sample, Fig. 4). Optimum material performance is obtained when stitching is kept as loose as practicable.

Flight evaluation of the heat shield (Fig. 1) will be conducted shortly on a Thor-boosted Delta vehicle. In-flight temperature measurements will be made, and the results of the measurements will be reported in a subsequent article.

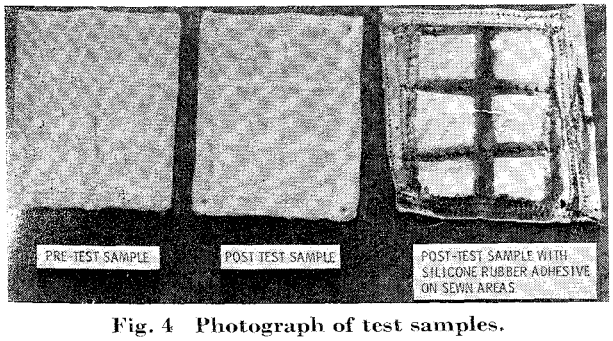

Fig. 4 Photograph of test samples.

References

[1] Property Bulletin 310-30, Industrial Glass Fabrics Department, J. P. Stevens and Co. Inc.

[2] "Refractory Fibrous Materials, Fiberfrax Specification," DS-5R 1064, March 1966, The Carborundum Co., Refractories Div.

[3] Hodgman, C. D., *Handbook of Chemistry and Physics*, Chemical Rubber Publishing Co., Cleveland, 1959.

[4] Gubareff, G. G., Janssen, J. R., and Torborg, R. H., *Thermal Radiation Properties Survey*, Minneapolis, Honeywell Research Center, 1960.

Helium Injection to Reduce Resonant Frequencies in Propellant Lines

Brantley R. Hanks* and David G. Stephens†
NASA Langley Research Center,
Langley Station, Hampton, Va.

LIQUID propellant launch vehicles often encounter severe longitudinal oscillations (accordianlike or "pogo" motion) during flight as a result of a closed-loop coupling of vibrations in the structure, propellant feed system, and engine.[1,2] One proposed "fix" is to alter the resonant frequencies of the propellant feed system by injecting small amounts of gas into the flowing liquid to decrease the speed of sound in the liquid. The lowering of sound velocity by gas bubbles in a liquid has been reported by others.[3,4] The objective of the program discussed herein was to study the change in resonant frequencies and resonant pressure responses resulting from the addition of helium to water flow lines in both normal and increased acceleration fields.

Apparatus, Test Procedure, and Analysis

The test apparatus (Figs. 1 and 2) consisted of an overhead 3-ft-diam, 8-ft-high pressurized water tank on a nonrotating foundation with a feed line running through a rotary gland and flexible rubber feed pipe to a test section mounted radially on a whirl table. The whirl table was used to produce a nominal 3.4g acceleration field on the test section to simulate a typical flight acceleration condition. The test section was a 17-ft-long, 1.5-in.-i.d., 2-in.-o.d., stainless-steel tube that had a 3-in.-diam cylinder and piston attached at its near end at the center of the whirl table. The piston was driven by a hydraulic shaker which was controlled to sweep frequency at a uniform (1 decade/min) rate at constant acceleration for frequencies above 20 Hz and at constant amplitude below 20 Hz. Water flowed into the test section from the tank above through a Y-joint just ahead of the piston

Presented at the AIAA Structural Dynamics and Aeroelasticity Specialist Conference, New Orleans, La., April 16–17, 1969 (no paper number; published in bound volume of conference papers); submitted May 16, 1969; revision received July 22, 1969.

* Aerospace Engineer. Associate AIAA.
† Head, Environmental Systems Section. Member AIAA.